



The C-Terminal RRM/ACT Domain Is Crucial for Fine-Tuning the Activation of ‘Long’ RelA-SpoT Homolog Enzymes by Ribosomal Complexes

Hiraku Takada^{1,2*}, Mohammad Roghanian^{1,2}, Victoriia Murina^{1,2}, Ievgen Dzhygyr^{1,2}, Rikinori Murayama³, Genki Akanuma⁴, Gemma C. Atkinson¹, Abel Garcia-Pino^{5,6} and Vasili Haurlyliuk^{1,2,7*}

¹ Department of Molecular Biology, Umeå University, Umeå, Sweden, ² Laboratory for Molecular Infection Medicine Sweden, Umeå University, Umeå, Sweden, ³ Akita Prefectural Research Center for Public Health and Environment, Akita, Japan, ⁴ Department of Life Science, Graduate School of Science, Gakushuin University, Tokyo, Japan, ⁵ Cellular and Molecular Microbiology, Faculté des Sciences, Université Libre de Bruxelles, Brussels, Belgium, ⁶ WELBIO, Brussels, Belgium, ⁷ Institute of Technology, University of Tartu, Tartu, Estonia

OPEN ACCESS

Edited by:

Michael Cashel,
Eunice Kennedy Shriver National
Institute of Child Health and Human
Development (NICHD), United States

Reviewed by:

Rebecca Corrigan,
University of Sheffield,
United Kingdom
Christiane Wolz,
University of Tübingen, Germany

*Correspondence:

Hiraku Takada
hiraku.takada@umu.se
Vasili Haurlyliuk
vasili.haurlyliuk@umu.se

Specialty section:

This article was submitted to
Microbial Physiology and Metabolism,
a section of the journal
Frontiers in Microbiology

Received: 21 November 2019

Accepted: 06 February 2020

Published: 28 February 2020

Citation:

Takada H, Roghanian M,
Murina V, Dzhygyr I, Murayama R,
Akanuma G, Atkinson GC,
Garcia-Pino A and Haurlyliuk V (2020)
The C-Terminal RRM/ACT Domain Is
Crucial for Fine-Tuning the Activation
of ‘Long’ RelA-SpoT Homolog
Enzymes by Ribosomal Complexes.
Front. Microbiol. 11:277.
doi: 10.3389/fmicb.2020.00277

The (p)ppGpp-mediated stringent response is a bacterial stress response implicated in virulence and antibiotic tolerance. Both synthesis and degradation of the (p)ppGpp alarmone nucleotide are mediated by RelA-SpoT Homolog (RSH) enzymes which can be broadly divided in two classes: single-domain ‘short’ and multi-domain ‘long’ RSH. The regulatory ACT (Aspartokinase, Chorismate mutase and TyrA)/RRM (RNA Recognition Motif) domain is a near-universal C-terminal domain of long RSHs. Deletion of RRM in both monofunctional (synthesis-only) RelA as well as bifunctional (i.e., capable of both degrading and synthesizing the alarmone) Rel renders the long RSH cytotoxic due to overproduction of (p)ppGpp. To probe the molecular mechanism underlying this effect we characterized *Escherichia coli* RelA and *Bacillus subtilis* Rel RSHs lacking RRM. We demonstrate that, first, the cytotoxicity caused by the removal of RRM is counteracted by secondary mutations that disrupt the interaction of the RSH with the starved ribosomal complex – the ultimate inducer of (p)ppGpp production by RelA and Rel – and, second, that the hydrolytic activity of Rel is not abrogated in the truncated mutant. Therefore, we conclude that the overproduction of (p)ppGpp by RSHs lacking the RRM domain is not explained by a lack of auto-inhibition in the absence of RRM or/and a defect in (p)ppGpp hydrolysis. Instead, we argue that it is driven by misregulation of the RSH activation by the ribosome.

Keywords: ppGpp, Rel, ACT, RRM, stringent response, ribosome

INTRODUCTION

Bacteria employ diverse mechanisms to sense and respond to stress. One such mechanism is the stringent response – a near-universal stress response orchestrated by hyper-phosphorylated derivatives of housekeeping nucleotides GDP and GTP: guanosine tetrphosphate (ppGpp) and guanosine pentaphosphate (pppGpp), collectively referred to as (p)ppGpp (Haurlyliuk et al., 2015; Liu et al., 2015; Steinchen and Bange, 2016). Since the stringent response and (p)ppGpp-mediated

signaling are implicated in virulence, antibiotic resistance and tolerance (Dalebroux et al., 2010; Dalebroux and Swanson, 2012; Hauryliuk et al., 2015), this stress signaling system has been recently targeted for development of new anti-infective compounds (Kushwaha et al., 2019).

Both synthesis and degradation of (p)ppGpp is mediated by RelA/SpoT Homolog (RSH) enzymes. RSHs can be broadly divided into two classes: 'long' multi-domain and 'short' single-domain factors (Atkinson et al., 2011; Jimmy et al., 2019). In the majority of bacteria, including model Gram-positive bacterial species *Bacillus subtilis*, the long multi-domain RSHs are represented by one bifunctional enzyme, Rel (Mittenhuber, 2001; Atkinson et al., 2011). Beta- and Gammaproteobacteria, such as *Escherichia coli*, encode two long RSH factors – RelA and SpoT – which are the products of gene duplication and diversification of the ancestral *rel* stringent factor (Mittenhuber, 2001; Atkinson et al., 2011; Hauryliuk et al., 2015). *E. coli* RelA is the most well-studied long RSH. RelA is a dedicated sensor of amino acid starvation with strong (p)ppGpp synthesis activity that is induced by ribosomal complexes harboring cognate deacylated tRNA in the A-site, so-called 'starved' ribosomal complexes (Haseltine and Block, 1973). Unlike RelA, which lacks (p)ppGpp hydrolysis activity (Shyp et al., 2012), Rel and SpoT can both synthesize and degrade (p)ppGpp (Xiao et al., 1991; Avarbock et al., 2000). Similarly to RelA – and to the exclusion of SpoT – (p)ppGpp synthesis by Rel is strongly activated by starved ribosomes (Avarbock et al., 2000). In addition to long RSHs, bacteria often encode single domain RSH enzymes: Small Alarmone Synthetases (SAS) and Small Alarmone Hydrolases (SAH) (Atkinson et al., 2011; Jimmy et al., 2019), such as RelQ and RelP in the Firmicute bacterium *B. subtilis* (Nanamiya et al., 2008).

Long RSHs are universally comprised of two functional regions: the catalytic N-terminal domains (NTD) and the regulatory C-terminal domains (CTD) (Figure 1A) (Atkinson et al., 2011). The NTD region comprises the (p)ppGpp hydrolase domain (HD; enzymatically inactive in RelA) and the (p)ppGpp synthetase domain (SYNTH) linked by an α -helical region that regulates the allosteric crosstalk between both domains (Tamman et al., 2019). The CTD encompasses four domains: the Thr-tRNA synthetase, GTPase and SpoT domain (TGS), the Helical domain, the Zing Finger Domain (ZFD) [equivalent to Ribosome-InterSubunit domain, RIS, as per (Loveland et al., 2016), or Conserved Cysteine, CC, as per (Atkinson et al., 2011)], and, finally, the RNA Recognition Motif domain (RRM) [equivalent to Aspartokinase, Chorismate mutase and TyrA, ACT, as per (Atkinson et al., 2011)]. When Rel/RelA is bound to a starved ribosomal complex, the TGS domain inspects the deacylated tRNA in the A-site and the TGS domain interacts directly with the 3' CCA end of the A-site tRNA (Arenz et al., 2016; Brown et al., 2016; Loveland et al., 2016). The conserved histidine 432 residue of *E. coli* RelA mediating this interaction is crucial for activation of RelA's enzymatic activity by the 3' CCA (Winther et al., 2018). Both ZFD and RRM interact with the A-site finger (ASF) of the 23S ribosomal RNA (Arenz et al., 2016; Brown et al., 2016; Loveland et al., 2016), and in *E. coli* RelA this

contact is crucial for efficient recruitment to and activation by starved ribosomal complexes (Kudrin et al., 2018).

While the NTD is responsible for the enzymatic function of RSHs, the CTD senses the starved ribosomal complex and transmits the signal to activate NTD-mediated (p)ppGpp synthesis by Rel/RelA (Agirrezabala et al., 2013; Arenz et al., 2016; Brown et al., 2016; Loveland et al., 2016). Since removal of the CTD increases the rate of (p)ppGpp production by Rel/RelA in the absence of ribosomes or starved complexes, the CTD was proposed to mediate the auto-inhibition of the NTD synthetase activity, thus precluding uncontrolled production of cytotoxic (p)ppGpp (Schreiber et al., 1991; Gropp et al., 2001; Mechold et al., 2002; Avarbock et al., 2005; Jiang et al., 2007; Yang et al., 2019).

The specific focus of this study is the C-terminal RRM/ACT domain of ribosome-associated RSH RelA and Rel. The RRM is absent in RelA enzymes from *Methylotenera mobilis*, *Elusimicrobium minutum*, *Francisella philomiraga*, and *Francisella tularensis* (Atkinson et al., 2011). The only experimentally characterized representative amongst these is *F. tularensis* RelA (Wilkinson et al., 2015). In a reconstituted biochemical system, the factor behaves similarly to *E. coli* RelA, i.e., it has very low synthesis activity by itself and is potently activated by the ribosome. Conversely, deletion of the RRM domain in factors that naturally possess it leads to inhibition of growth (Gratani et al., 2018; Ronneau et al., 2019; Turnbull et al., 2019) that is mediated by over-production of (p)ppGpp in the cell, as shown for *Caulobacter crescentus* Rel (Ronneau et al., 2019) and *E. coli* RelA (Turnbull et al., 2019). The exact molecular mechanism of misregulation remains unclear. Deletion of RRM in bifunctional *C. crescentus* Rel leads to compromised hydrolase activity (Ronneau et al., 2019), while overproduction of (p)ppGpp by monofunctional *E. coli* RelA Δ RRM was suggested to be due to upregulated constitutive synthesis activity, conceivably due to defective auto-inhibition of the NTD synthetase domain by the CTD (Turnbull et al., 2019).

In this report, we inspected the possible role of the ribosome in overproduction of (p)ppGpp by Δ RRM variants of long RSHs in the cell. By characterizing truncated versions of *E. coli* RelA and *B. subtilis*, we demonstrate that the cytotoxicity of mutant RSH variants is strictly dependent on the interaction with the ribosome and deacylated tRNA, and, therefore, cannot be explained by defects in intra-molecular regulation alone.

MATERIALS AND METHODS

Multiple Sequence Alignment

Sequences were aligned with MAFFT v7.164b with the L-INS-i strategy (Katoh and Standley, 2013), and alignments were visualized with Jalview (Waterhouse et al., 2009).

Construction of Bacterial Strains and Plasmids

The strains and plasmids used in this study are listed in **Supplementary Tables S1–S3**. Oligonucleotides used in this study are provided in **Supplementary Table S4**.

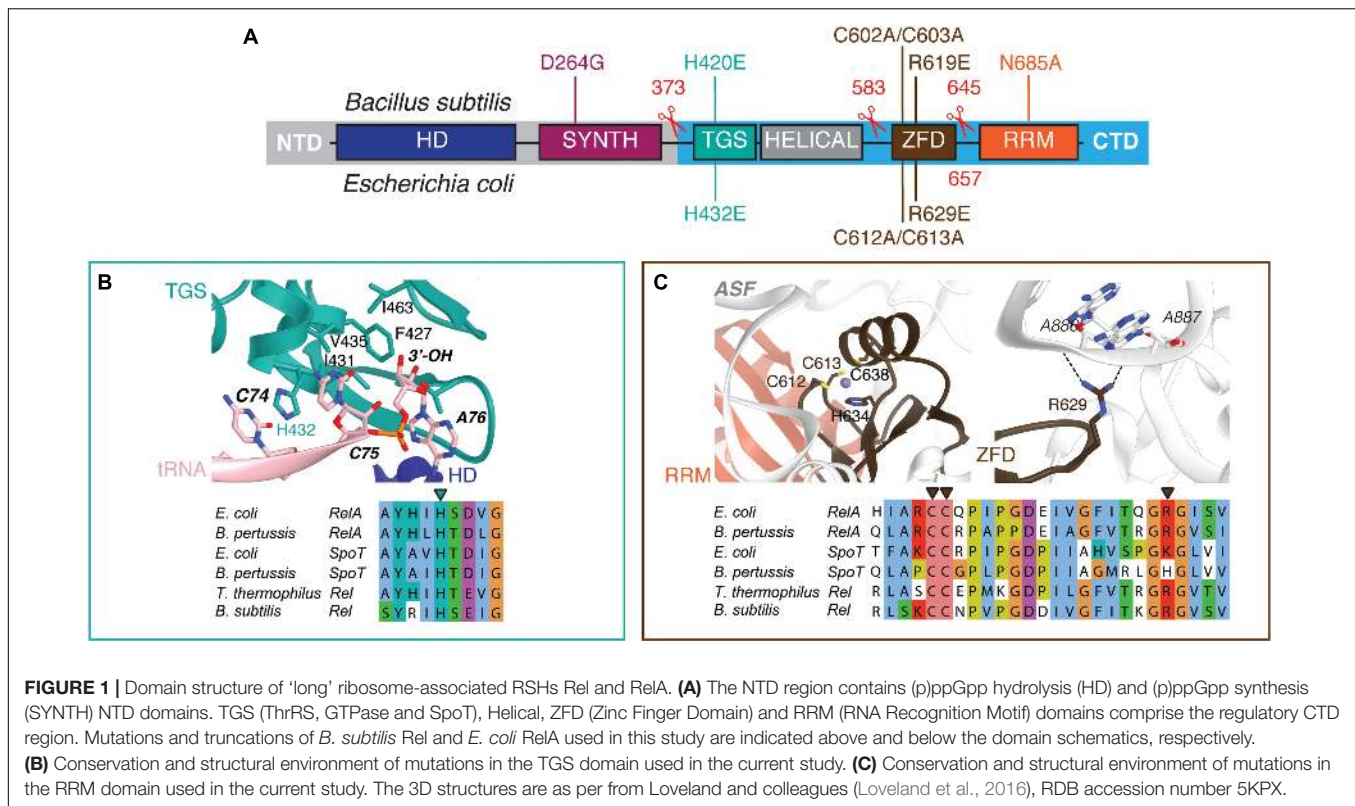


FIGURE 1 | Domain structure of 'long' ribosome-associated RSHs Rel and RelA. **(A)** The NTD region contains (p)ppGpp hydrolysis (HD) and (p)ppGpp synthesis (SYNTH) NTD domains. TGS (ThrRS, GTPase and SpoT), Helical, ZFD (Zinc Finger Domain) and RRM (RNA Recognition Motif) domains comprise the regulatory CTD region. Mutations and truncations of *B. subtilis* Rel and *E. coli* RelA used in this study are indicated above and below the domain schematics, respectively. **(B)** Conservation and structural environment of mutations in the TGS domain used in the current study. **(C)** Conservation and structural environment of mutations in the RRM domain used in the current study. The 3D structures are as per from Loveland and colleagues (Loveland et al., 2016), RDB accession number 5KPX.

A detailed description of strain construction is provided in the **Supplementary Material**.

Growth Assays

Escherichia coli BW25113 cells were transformed with expression constructs either based on a high-copy IPTG inducible vector pUC derivative pMG25 (pMG25:relA, Turnbull et al., 2019, pMG25:relA^{ΔRRM}, pMG25:spoR or pMG25:spoT^{ΔRRM}) or on a low-copy IPTG inducible vector, mini R1 plasmid pNDM220 which is present in one to two copies per chromosome (Molin et al., 1979) (pNDM220:relA, pNDM220:relA^{ΔRRM}, pNDM220:relA^{ΔRRM-H432E}, pNDM220:relA^{ΔRRM-R629E} or pNDM220:relA^{ΔRRM-C612A/C613A}). For solid medium growth assays, ten-fold serial dilutions of overnight LB cultures were spotted onto LB agar supplemented with 30 μg/mL ampicillin and 1 mM IPTG. For liquid medium growth assays, 1000-fold dilutions of the overnight LB cultures were made in liquid LB supplemented with 30 μg/mL ampicillin and 1 mM IPTG, seeded on a 100-well honeycomb plate (Oy Growth Curves AB Ltd, Helsinki, Finland), and plates incubated in a Bioscreen C (Labsystems, Helsinki, Finland) at 37°C with continuous medium shaking.

Bacillus subtilis strains were pre-grown on LB plates lacking the IPTG inducer overnight (10 h) at 30°C. Fresh individual colonies were used to inoculate filtered LB medium in the presence of indicated concentrations of IPTG and OD₆₀₀ adjusted to 0.01. The cultures were seeded on a 100-well honeycomb plate (Oy Growth Curves AB Ltd, Helsinki, Finland), and plates were incubated in a

Bioscreen C (Labsystems, Helsinki, Finland) at 37°C with continuous medium shaking.

Growth rates (μ_2) were calculated as slopes of linear regression lines through log₂-transformed OD₆₀₀ data points.

Preparation of Polyclonal Anti-Rel Antiserum

The entire coding region of the *B. subtilis* rel gene was amplified by PCR using the synthetic oligonucleotide pQereA_F and pQereA_R containing a BamHI site and *B. subtilis* genomic DNA as a template. The resulting PCR fragment was cut with BamHI and then inserted into the BamHI sites of pQE60 (Qiagen), yielding plasmid pQereA. pQereA was transformed into *E. coli* M15 (pREP4) (Qiagen), fresh transformants were inoculated into LB liquid culture (1000 mL) with 100 μg/mL ampicillin and grown at 37°C with vigorous shaking. At OD₆₀₀ of 0.8 expression of Rel induced with 1 mM IPTG (final concentration). After 3 h of expression the cells were harvested by centrifugation, resuspended in buffer A (500 mM NaCl, 50 mM Tris-HCl pH 8.0) supplemented with 2 mM PMSF and lysed by sonication. Rel-His₆ inclusion bodies were collected by centrifugation, resuspended in buffer A supplemented with 8 M guanidine hydrochloride (= buffer B) and loaded onto an Ni-NTA agarose column (QIAGEN) pre-equilibrated in the same buffer. The column was washed with buffer B supplemented with 10 mM imidazole, and the protein was eluted with a 100–400 mM imidazole gradient in buffer B. The fractions containing Rel-His₆ was dialyzed against buffer A at 4°C overnight. Aggregated

Rel-His₆ protein was collected by centrifugation, resuspended in buffer A supplemented with 6 M urea and used for rabbit immunization. Rabbit serum was used as a polyclonal anti-Rel antibody.

Sucrose Gradient Fractionation and Western Blotting

Bacillus subtilis strains were pre-grown on LB plates overnight at 30°C. Fresh individual colonies were used to inoculate 200 mL LB cultures that were grown at 37°C. At OD₆₀₀ of 0.2 amino acid starvation was induced by addition of isoleucyl tRNA synthetase inhibitor mupirocin (dissolved in DMSO, AppliChem) to final concentration of 700 nM for 20 min. As a mock control, a separate culture was treated with the same amount of DMSO. After 20 min the cells were collected by centrifugation (8,000 rpm, 5 min, JLA-16.25 Beckman Coulter rotor), dissolved in 0.5 mL of HEPES:Polymix buffer [5 mM Mg(OAc)₂] supplemented with 2 mM PMSF, lysed using FastPrep homogenizer (MP Biomedicals) by four 20 s pulses at speed 6.0 mp/s with chilling on ice for 1 min between the cycles), and clarified by ultracentrifugation (14,800 rpm for 20 min, Microfuge 22R centrifuge Beckman Coulter, F241.5P rotor). Clarified cell lysates were loaded onto 10–35% sucrose gradients in HEPES:Polymix buffer pH 7.5 (5 mM Mg²⁺ final concentration), subjected to centrifugation (36,000 rpm for 3 h at 4°C, SW-41Ti Beckman Coulter rotor) and analyzed using Biocomp Gradient Station (BioComp Instruments) with A₂₆₀ as a readout.

For Western blotting 0.5 mL fractions were supplemented with 1.5 mL of 99.5% ethanol, precipitated overnight at –20°C. After centrifugation at 14,800 rpm for 30 min at 4°C the supernatants were discarded and the samples were dried. The pellets were resuspended in 40 µL of 2xSDS loading buffer [100 mM Tris-HCl pH 6.8, 4% SDS (w/v) 0.02% Bromophenol blue, 20% glycerol (w/v) 4% β-mercaptoethanol], resolved on the 8% SDS PAGE and transferred to nitrocellulose membrane (Trans-Blot Turbo Midi Nitrocellulose Transfer Pack, Bio-Rad, 0.2 µm pore size) with the use of a Trans-Blot Turbo Transfer Starter System (Bio-Rad) (10 min, 2.5 A, 25 V). Membrane blocking was done for 1 h in PBS-T (1xPBS 0.05% Tween-20) with 5% w/v non-fat dry milk at room temperature. Rel was detected using anti-Rel primary combined with goat anti-rabbit IgG-HRP secondary antibodies. All antibodies were used at 1:10,000 dilution. ECL detection was performed using WesternBright™ Quantum (K-12042-D10, Advantia) Western blotting substrate and an ImageQuant LAS 4000 (GE Healthcare) imaging system.

Expression and Purification of *E. coli* RelA and *B. subtilis* Rel

Wild type and H432E mutant variants of *E. coli* RelA were expressed and purified as described earlier (Turnbull et al., 2019).

Wild type and mutant variants of *B. subtilis* Rel were overexpressed in freshly transformed *E. coli* BL21 DE3 Rosetta (Novagen). Fresh transformants were inoculated to final OD₆₀₀ of 0.05 in the LB medium (800 mL) supplemented with 100 µg/mL kanamycin. The cultures were grown at 37°C until an OD₆₀₀

of 0.5, induced with 1 mM IPTG (final concentration) and grown for additional 1.5 h at 30°C. The cells were harvested by centrifugation and resuspended in buffer A (750 mM KCl, 5 mM MgCl₂, 40 µM MnCl₂, 40 µM Zn(OAc)₂, 1 mM mellitic acid (Tokyo Kasei Kogyo Co., Ltd.), 20 mM imidazole, 10% glycerol, 4 mM β-mercaptoethanol, 25 mM HEPES:KOH pH 8) supplemented with 0.1 mM PMSF and 1 U/mL of DNase I. Cells were lysed by one passage through a high-pressure cell disrupter (Stansted Fluid Power, 150 MPa), cell debris was removed by centrifugation (25,000 rpm for 40 min, JA-25.50 Beckman Coulter rotor) and clarified lysate was taken for protein purification.

To prevent possible substitution of Zn²⁺ ions in Rel's Zn-finger domain for Ni²⁺ during purification on an Ni-NTA metal affinity chromatography column (Block et al., 2009), a 5 mL HisTrap HP column was stripped from Ni²⁺ in accordance with manufacturer's recommendations, washed with 5 column volumes (CV) of 100 mM Zn(OAc)₂ pH 5.0 followed by 5 CV of deionized water. Clarified cell lysate was filtered through a 0.2 µm syringe filter and loaded onto the Zn²⁺-charged HisTrap 5 mL HP column pre-equilibrated in buffer A. The column was washed with 5 CV of buffer A, and the protein was eluted with a linear gradient (6 CV, 0–100% buffer B) of buffer B (750 mM KCl, 5 mM MgCl₂, 40 µM MnCl₂, 40 µM Zn(OAc)₂, 1 mM mellitic acid, 500 mM imidazole, 10% glycerol, 4 mM β-mercaptoethanol, 25 mM HEPES:KOH pH 8). Mellitic acid forms highly ordered molecular networks when dissolved in water (Inabe, 2005) and it was shown to promote the stability of *Thermus thermophilus* Rel (Van Nerom et al., 2019). Fractions most enriched in Rel (≈25–50% buffer B) were pooled, totaling approximately 5 mL. The sample was loaded on a HiLoad 16/600 Superdex 200 pg column pre-equilibrated with a high salt buffer (buffer C; 2 M NaCl, 5 mM MgCl₂, 10% glycerol, 4 mM β-mercaptoethanol, 25 mM HEPES:KOH pH 8). The fractions containing Rel were pooled and applied on HiPrep 10/26 desalting column (GE Healthcare) pre-equilibrated with storage buffer (buffer D; 720 mM KCl, 5 mM MgCl₂, 50 mM arginine, 50 mM glutamic acid, 10% glycerol, 4 mM β-mercaptoethanol, 25 mM HEPES:KOH pH 8). Arginine and glutamic acid were added to improve protein solubility and long-term stability (Golovanov et al., 2004). The fractions containing Rel were collected and concentrated in an Amicon Ultra (Millipore) centrifugal filter device (cut-off 50 kDa). To cleave off the His₁₀-SUMO tag, 35 µg of His₆-Ulp1 per 1 mg of Rel were added and the reaction mixture was incubated at room temperature for 15 min. After the His₁₀-SUMO tag was cleaved off, the protein was passed through 5 mL Zn²⁺-charged HisTrap HP pre-equilibrated with buffer D. Fractions containing Rel in the flow-through were collected and concentrated on Amicon Ultra (Millipore) centrifugal filter device with 50 kDa cut-off. The purity of protein preparations was assessed by SDS-PAGE and spectrophotometrically [OD₂₆₀/OD₂₈₀ ratio below 0.8 corresponding to less than 5% RNA contamination (Layne, 1957)]. Protein preparations were aliquoted, frozen in liquid nitrogen and stored at –80°C. Individual single-use aliquots were discarded after the experiment.

Negative Staining Electron Microscopy

3.5 μ L of 2 μ M Rel protein was loaded onto a glow-discharged Cu₃₀₀ grid (TAAB Laboratories Equipment Ltd.) with manually layered 2.9 nm carbon. The sample was incubated on the grid for 1–3 min, blotted with Watman filter paper, than twice washed with water and blotted, stained with 1.5% uranyl acetate pH 4.2 for 30 s before the final blotting. Grids were dried on the bench and imaged by Talos L 120C (FEI) microscope with 92,000X magnification.

Preparation of 10X Polymix Buffer Base

The 10X Polymix base was prepared as per (Antoun et al., 2004), with minor modifications. For preparation of the putrescine solution, 100 g of putrescine (1,4-diaminobutane) was dissolved in 600 mL of ddH₂O at 90°C, and the pH adjusted with acetic acid to 8.0 (approximately 100 mL of 100% acetic acid). After cooling to room temperature, the pH was adjusted further to 7.6 and the volume was adjusted to the final of 2 L by addition of 1.134 L of ddH₂O. One 100 mL cup of activated charcoal was added and the slurry was stirred under the hood for 30 min. The slurry was filtered through, first, Whatman paper and then through a 0.45 μ m BA85 membrane. The final solution was stored at 4°C in a bottle wrapped in foil since putrescine is photosensitive. The preparation of 2 L of 10X Polymix buffer base used 141.66 g KCl, 5.35 g NH₄Cl, 21.44 g Mg(OAc)₂·4H₂O, 1.47 g CaCl₂·2H₂O, 5.092 g spermidine, and 160 ml of putrescine solution (described above). The salts were dissolved in ddH₂O (\approx 1,500 mL), then the putrescine solution was added and mixed well. Spermidine was dissolved in a small volume of ddH₂O and added to the mixture. The pH was adjusted to 7.5 with concentrated acetic acid or 5 M KOH, and after that the volume was adjusted by adding ddH₂O to 2 L. The buffer was filtered through 0.2 μ m nitrocellulose filter (2–3 filters are needed). The resulting 10X Polymix buffer base was aliquoted and stored at –20°C. The final working HEPES:Polymix buffer was made using the 10X Polymix buffer base, 1M DDT and 1 M HEPES:KOH pH 7.5 and contains 20 mM HEPES:KOH pH 7.5, 2 mM DTT, 5 mM MgOAc₂, 95 mM KCl, 5 mM NH₄Cl, 0.5 mM CaCl₂, 8 mM putrescine, 1 mM spermidine.

Purification of *B. subtilis* 70S Ribosomes

Bacillus subtilis strain RIK2508 (*trpC2* Δ *hpf*) strain (Akanuma et al., 2016; Brodiazhenko et al., 2018) was pre-grown on LB plates overnight at 30°C. Fresh individual colonies were used to inoculate LB liquid cultures (25 \times 400 mL) to OD₆₀₀ of 0.05 and grown at 37°C with vigorous shaking. At OD₆₀₀ 1.2 the cells were pelleted at 4°C (TLA10.500 (Beckman), 15 min at 5,000–8,000 rcf), resuspended with ice-cold PBS buffer, pelleted again in 50 mL Falcon tubes, frozen with liquid nitrogen and stored at –80°C. Approximately 20 g of frozen *B. subtilis* cells were resuspended in 50 mL of cell opening buffer (100 mM NH₄Cl, 15 mM Mg(OAc)₂, 0.5 mM EDTA, 3 mM β -mercaptoethanol, 20 mM Tris:HCl pH 7.5) supplemented with 1 mU Turbo DNase (Thermo Fisher Scientific), 0.1 mM PMSF and 35 μ g/mL lysozyme, incubated on ice for 1 h, and opened by three passages on a high-pressure cell disrupter (Stansted Fluid Power) at

220 MPa. Lysed cells were clarified by centrifugation for 40 min at 40,000 rpm (Ti 45 rotor, Beckman), NH₄Cl concentration was adjusted to 400 mM, and the mixture was filtered through 0.45 μ m syringe filters. The filtrated lysate was loaded onto a pre-equilibrated 80 mL CIMmultus QA-80 column (BIA Separations, quaternary amine advanced composite column) at a flow rate of 20 mL/min, and the column washed with 5 CV (CV = 80 mL) of low salt buffer [400 mM NH₄Cl, 15 mM Mg(OAc)₂, 3 mM β -mercaptoethanol, 20 mM Tris:HCl pH 7.5]. Ribosomes were then eluted in 45 mL fractions by a step gradient to 77% high salt buffer [900 mM NH₄Cl, 15 mM Mg(OAc)₂, 3 mM β -mercaptoethanol, 20 mM Tris:HCl pH 7.5] for 5 CV, followed by 100% high salt buffer for 1 CV. The fractions containing ribosomes were pooled, the concentration of NH₄Cl was adjusted to 100 mM, and the ribosomes were treated with puromycin added to a final concentration of 10 μ M. The resultant crude 70S preparation was resolved on a 10–40% sucrose gradient in overlay buffer [60 mM NH₄Cl, 15 mM Mg(OAc)₂, 0.25 mM EDTA, 3 mM β -mercaptoethanol, 20 mM Tris:HCl pH 7.5] in a zonal rotor (Ti 15, Beckman, 17 h at 21,000 rpm). The peak containing pure 70S ribosomes was pelleted by centrifugation (20 h at 35,000 rpm), and the final ribosomal preparation was dissolved in HEPES:Polymix buffer [20 mM HEPES:KOH pH 7.5, 2 mM DTT, 5 mM Mg(OAc)₂, 95 mM KCl, 5 mM NH₄Cl, 0.5 mM CaCl₂, 8 mM putrescine, 1 mM spermidine (Antoun et al., 2004)]. 70S concentration was measured spectrophotometrically (1 OD₂₆₀ corresponds to 23 nM of 70S) and ribosomes were aliquoted (50–100 μ L per aliquot), snap-frozen in liquid nitrogen and stored at –80°C.

Preparation of 70S Initiation Complexes (70S IC)

Initiation complexes were prepared by as per (Murina et al., 2018a,b), with minor modifications. The reaction mix containing *B. subtilis* 70S ribosomes (final concentration of 6 μ M) with *E. coli* IF1 (4 μ M), IF2 (5 μ M), IF3 (4 μ M), ³H-fMet-tRNA^{fMet} (8 μ M), mRNA MVFStop (8 μ M, 5'-GGCAAGGAGGAGUAAGAAUGGUUUUCUAAUA-3'; Shine-Dalgarno sequence is highlighted in bold, ORF is underlined), 1 mM GTP and 2 mM DTT in 1 \times HEPES:Polymix buffer [20 mM HEPES:KOH pH 7.5, 95 mM KCl, 5 mM NH₄Cl, 5 mM Mg(OAc)₂, 0.5 mM CaCl₂, 8 mM putrescine, 1 mM spermidine, 1 mM DTT (Antoun et al., 2004)] was incubated at 37°C for 30 min. Then the ribosomes were pelleted through a sucrose cushion (1.1 M sucrose in HEPES:Polymix buffer with 15 mM Mg²⁺) at 50,000 rpm for 2 h (TLS-55, Beckman), the pellet was dissolved in HEPES:Polymix buffer [5 mM Mg(OAc)₂], aliquoted, frozen in liquid nitrogen and stored at –80°C.

Preparation of ³H-Labeled pppGpp

3 μ M *E. faecalis* RelQ (Beljantseva et al., 2017) was incubated in reaction buffer (18 mM MgCl₂, 20 mM DTT, 20 mM Tris:HCl pH 8.0) together with 8 mM ATP and 5 mM ³H-GTP (SA: 100 cpm/pmol) for 2 h at 37°C to produce ³H-pppGpp. The resultant mixture was loaded on strong anion-exchange column (MonoQ 5/50 GL; GE Healthcare), and nucleotides were resolved

by a 0.5–1,000 mM LiCl gradient. Peak fractions containing ^3H -pppGpp were pooled and precipitated by addition of lithium chloride to a final concentration of 1 M followed by addition of four volumes of ethanol. The suspension was incubated at -80°C overnight and centrifuged (14,800 rpm, 30 min, 4°C). The resulting pellets were washed with absolute ethanol, dried, dissolved in 20 mM HEPES-KOH buffer (pH 7.5) and stored at -80°C .

^3H -pppGpp Hydrolysis Assay

The reaction mixtures contained 140–250 nM Rel, 300 μM ^3H -pppGpp, 1 mM MnCl_2 , an essential cofactor for Rel's hydrolysis activity (Avarbock et al., 2000; Mechold et al., 2002; Tamman et al., 2019), all in HEPES:Polymix buffer (5 mM Mg^{2+} final concentration). After preincubation at 37°C for 3 min, the reaction was started by the addition of prewarmed Rel and 5 μL aliquots were taken throughout the time course of the reaction and quenched with 4 μL 70% formic acid supplemented with a cold nucleotide standard (4 mM GTP) for UV-shadowing.

^3H -pppGpp Synthesis Assay

Assays with *E. coli* RelA were performed as described earlier (Kudrin et al., 2018). In the case of *B. subtilis* Rel, the reaction mixtures typically contained 500 nM *B. subtilis* 70S IC(MVF), 140 nM Rel, guanosine nucleoside substrate (300 μM ^3H -GTP, PerkinElmer), 100 μM pppGpp, 2 μM *E. coli* tRNA^{Val} (ChemBlock), all in HEPES:Polymix buffer (5 mM Mg^{2+} final concentration). After preincubation at 37°C for 3 min, the reaction was started by the addition of prewarmed ATP to the final concentration of 1 mM, and 5 μL aliquots were taken throughout the time course of the reaction and quenched with 4 μL 70% formic acid supplemented with a cold nucleotide standard (4 mM GTP) for UV-shadowing. Individual quenched timepoints were spotted PEI-TLC plates (Macherey-Nagel) and nucleotides were resolved in 1.5 M KH_2PO_4 pH 3.5 buffer. The TLC plates were dried, cut into sections as guided by UV-shadowing, and ^3H radioactivity was quantified by scintillation counting in EcoLite Liquid Scintillation Cocktail (MP Biomedicals).

RESULTS

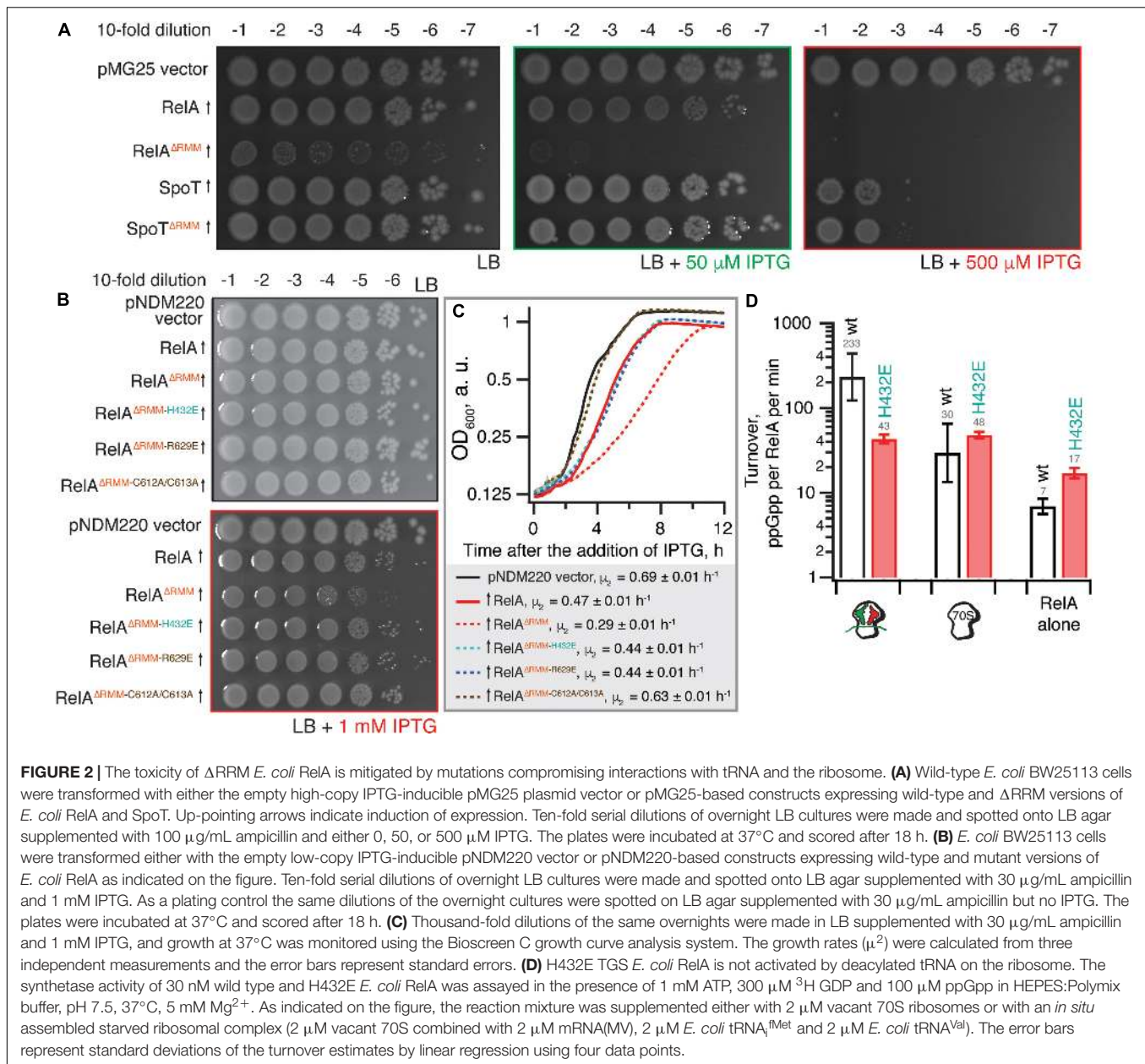
Toxicity of *E. coli* ΔRRM RelA Is Countered by Mutations Compromising the Interaction With Starved Ribosomes

As we have shown earlier, low-level ectopic expression of RelA $^{\Delta\text{RRM}}$ from a low copy number pNDM220 plasmid under the control of a $\text{P}_{\text{A1/04/03}}$ promoter has a more pronounced inhibitory effect on *E. coli* growth in comparison with expression of the full-length protein (Turnbull et al., 2019). We tested whether $\text{P}_{\text{A1/04/03}}$ -driven high-level expression of RelA $^{\Delta\text{RRM}}$ from a high-copy pUC derivative pMG25 would cause a more pronounced growth defect (Figure 2A). For comparison, we tested the effects of expression of the second *E. coli* RSH enzyme – SpoT – using both the full-length and the ΔRRM variants.

Even in the absence of the IPTG inducer, leaky expression of RelA $^{\Delta\text{RRM}}$ has a dramatic effect on *E. coli* growth, while the full-length protein does not have an effect. In the presence of 50 μM IPTG, both full-length and RelA $^{\Delta\text{RRM}}$ inhibit the growth, although the latter has a stronger effect; induction with 500 μM IPTG completely abrogates the growth in both cases. While expression of SpoT has a detectable inhibitory effect at 500 μM IPTG, the effect is the same for full-length and SpoT $^{\Delta\text{RRM}}$. Since even leaky expression of RelA $^{\Delta\text{RRM}}$ inhibits growth, we concluded that this high-level expression system is ill-suited for follow-up microbiological investigations. Therefore, to test whether the toxicity of RelA $^{\Delta\text{RRM}}$ in *E. coli* is dependent on the interaction with starved complexes, we used the pNDM220-based low-level expression system used previously (Turnbull et al., 2019). Guided by the recent cryo-EM reconstructions of RelA (Arenz et al., 2016; Brown et al., 2016; Loveland et al., 2016), we designed a set of mutations that will specifically disrupt RelA's interaction with starved ribosomal complexes.

To disrupt the interaction between RelA and the tRNA, we adopted the H432E mutation in the TGS domain that was earlier shown to specifically abrogate the recognition of the 3' CCA end of the A/R tRNA (Winther et al., 2018). This conserved histidine residue stacks between the two cytosine bases and hydrogen-bonds the phosphodiester backbone (Figure 1B). Replacing it with glutamic acid introduces a charge repulsion effect as well as a steric clash. To disrupt the interaction with the ribosome we used mutations in the ZFD: R629E as well as a double substitution C602A C603A; both mutants are expected to compromise the recognition of the 23S rRNA ASF element that is crucial for RelA recruitment (Kudrin et al., 2018). The conserved double motif docks the ZFD α -helix into the major groove of the ASF; replacement by alanine is expected to abrogate this interaction (Figure 1C). The conserved arginine 629 residue is in close proximity to A886-A887 and A885-A886 phosphodiester bonds (3.5 and 5 Å, respectively), and, therefore, the R629E substitution is expected to cause electrostatic repulsion.

Low-level expression of full-length RelA has a minor, but detectable growth inhibitory effect both when tested on solid LB agar media (Figure 2B) and in liquid LB cultures [growth rate, μ_2 , decreases from 0.69 (vector) to 0.47 h^{-1}] (Figure 2C). Importantly, the spotting control on solid LB media lacking IPTG shows that the size of the inoculum is not affected by potential leaky expression in the overnight culture (Figure 2B). Deletion of the RRM renders RelA significantly more toxic (growth rate decreases to 0.29 h^{-1}), in good agreement with the accumulation of (p)ppGpp upon expression of the construct (Turnbull et al., 2019). The effect is countered by TGS H432E, ZFD R629E and even more so by the C612A C613A substitutions (Figures 2B,C). RelA $^{\Delta\text{RRM}}$ expression is equally toxic in the ΔrelA background and the effect is similarly countered by H432E, R629E and C612A C613A substitutions (Supplementary Figure S1), demonstrating that the growth inhibition is independent of the functionality of the endogenous RelA stringent factor. Finally, we directly confirmed the lack of activation by deacylated tRNA in the case of H432E *E. coli* RelA using biochemical assays (Figure 2D).



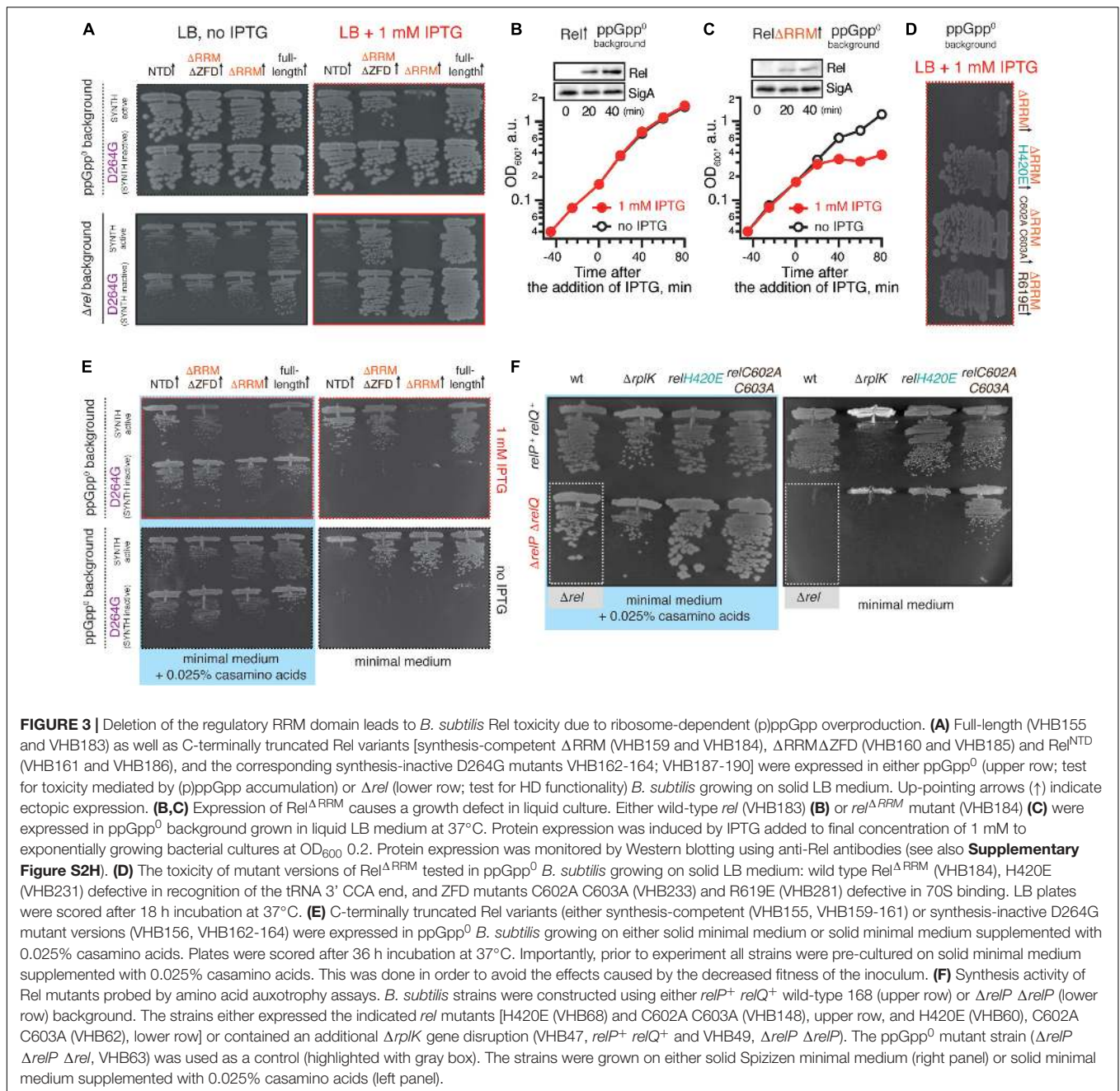
Taken together, our results suggest that RelA Δ RRM toxicity in *E. coli* is dependent on the functionality of the interaction with starved ribosomes. To test the generality of this hypothesis, we next characterized *B. subtilis* Rel lacking the RRM domain.

Toxicity of *B. subtilis* Δ RRM Rel Expressed in the ppGpp⁰ Background Is Mediated by (p)ppGpp Synthesis and Is Countered by Mutations Compromising the Interaction With Starved Ribosomes

We expressed Δ RRM Rel under the control of an IPTG-inducible *P*_{hy-spank} promoter (Britton et al., 2002) in ppGpp⁰ (Δ rel Δ relP Δ relQ) (Nanamiya et al., 2008) or Δ rel *B. subtilis*

strains (Figure 3A). In the ppGpp⁰ background, inhibition of *B. subtilis* growth on LB plates is a marker of toxic (p)ppGpp overproduction. In the Δ rel background, (p)ppGpp is overproduced by a SAS in the absence of Rel's hydrolytic activity, causing a growth defect in *B. subtilis* (Nanamiya et al., 2008) and *S. aureus* (Geiger et al., 2014). Therefore, this experiment tests the complementation of hydrolase function of Rel that manifests in improved growth.

Unlike the full-length Rel, the Rel Δ RRM truncation is toxic in the ppGpp⁰ and Δ rel backgrounds, both when the growth is followed on plates (Figure 3A) and in liquid culture (Figures 3B,C and Supplementary Figures S2A,B). To probe the role of the interactions with starved ribosomes in Rel Δ RRM toxicity, we used a set of substitutions in *B. subtilis* Rel



corresponding to those used to study *E. coli* RelA (Figures 1, 2). The toxicity of the Rel^{ARRM} mutant is efficiently countered by the H420E substitution in the TGS as well as the R619E and C602A C603A substitutions in the ZFD (Figure 3D and Supplementary Figures S2D–F,H). This strongly suggests that the intact interaction with tRNA and starved ribosomes is essential for the toxicity of Rel^{ARRM}. For comparison, we tested, full-length Rel, Rel^{ARRM} Δ ZFD C-terminal truncation, as well as the NTD domain region alone. The Rel^{ARRM} Δ ZFD mutant is only slightly toxic in the ppGpp⁰ background and its expression promotes growth in the Δ rel background (Figure 3A). NTD-alone construct displays no toxicity in the ppGpp⁰ background and does not promote the

growth in the Δ rel background, suggesting weak – or absent – synthetase activity.

To separate the effects of (p)ppGpp production from the effects of (p)ppGpp degradation, we tested synthesis-deficient SYNTH D264G mutants (Nanamiya et al., 2008) of C-terminally truncated Rel variants (Figure 3A and Supplementary Figure S2C). The toxicity of the Δ RRM variant is abolished by the D264G mutation demonstrating that it is, indeed, mediated by (p)ppGpp production and not, for example, through inhibition of protein synthesis via competitive binding to ribosomal A-site [the latter non-enzymatic mechanism of toxicity was shown for *E. coli* RelA^{CTD} (Turnbull et al., 2019)]. Both Δ RRM D264G

and $\Delta ZFD\Delta RRM$ D264G variants promote growth in the Δrel strain suggesting that neither deletion of ΔRRM alone – or both ΔZFD and ΔRRM – abrogates the hydrolysis activity of *B. subtilis* Rel (**Figure 3A**, bottom panel). At the same time expression of the synthesis-inactive D264G Rel^{NTD} has no effect, suggesting that the NTD does not efficiently hydrolyze (p)ppGpp. To test if further truncations of the NTD-only Rel (Rel^{1–373}) would induce hydrolytic activity, we tested several additional constructs of *B. subtilis* Rel – Rel^{1–336}, Rel^{1–196} and Rel^{1–155} – but neither of them could rescue the growth effect of Δrel *B. subtilis* (**Supplementary Figure S3**). Finally, the synthesis deficiency of D264G Rel and the lack of H420E Rel activation by deacylated tRNA was confirmed using biochemical assays (**Supplementary Figure S4**).

Taken together, our results demonstrate that (i) Rel ^{ΔRRM} is toxic in ppGpp⁰ *B. subtilis*, (ii) this toxicity requires intact (p)ppGpp synthesis activity of the enzyme (iii) it is abrogated by mutations disrupting the interaction with tRNA and starved ribosomes and (iv) deletion of the RRM domain does not abrogate the hydrolysis activity of *B. subtilis* Rel.

The Synthetase Activity of Rel ^{ΔRRM} , Rel ^{$\Delta RRM\Delta ZFD$} , and Rel^{NTD} but Not the Rel^{H420E} TGS Mutant Can Suppress Amino Acid Auxotrophy of ppGpp⁰ *B. subtilis*

To test the low-level, non-toxic, synthesis activity of Rel mutants and to validate the effects of point mutations disrupting the interaction of Rel with starved ribosomal complexes, we took advantage of the amino acid auxotrophy phenotype of the ppGpp⁰ *B. subtilis* ($\Delta rel \Delta relP \Delta relQ$) (Nanamiya et al., 2008).

When ppGpp⁰ *B. subtilis* is grown on Spizizen minimum medium (Spizizen, 1958) in the absence of casamino acids, neither of the D264G Rel mutants – either full-length or C-terminal truncations – promote growth, both whether or not expression is induced by 1 mM IPTG (**Figure 3E**, right panels). Full induction of NTD expression with 1 mM IPTG near-completely suppressed the auxotrophy phenotype (**Figure 3E**, top right panel), while the leaky expression in the absence of IPTG results in weak, but detectable suppression (**Figure 3E**, bottom right panel). This demonstrates that *B. subtilis* NTD has a weak net-synthesis activity. The Rel ^{ΔRRM} is, as expected, highly toxic when expression is induced by IPTG; conversely, low-level leakage expression efficiently suppresses the amino acid auxotrophy phenotype. Removal of both RRM and ZFD domains renders the protein non-toxic. It is not trivial to reconcile this effect with the idea that removal of the RRM renders the protein toxic due to lack of auto-inhibition: one would expect that the additional removal of the ZFD domain would further compromise the CTD-mediated negative control in Rel ^{ΔRRM} .

We next used the auxotrophy assay to test the effects of the H420E TGS and C602A C603A ZFD substitutions on the activity of Rel expressed from the native genomic locus under the control of the native promoter (**Figure 3F**). As a positive control we used a strain lacking the genomic copy of *rplK* (*relC*) encoding ribosomal protein L11. This ribosomal element is essential for

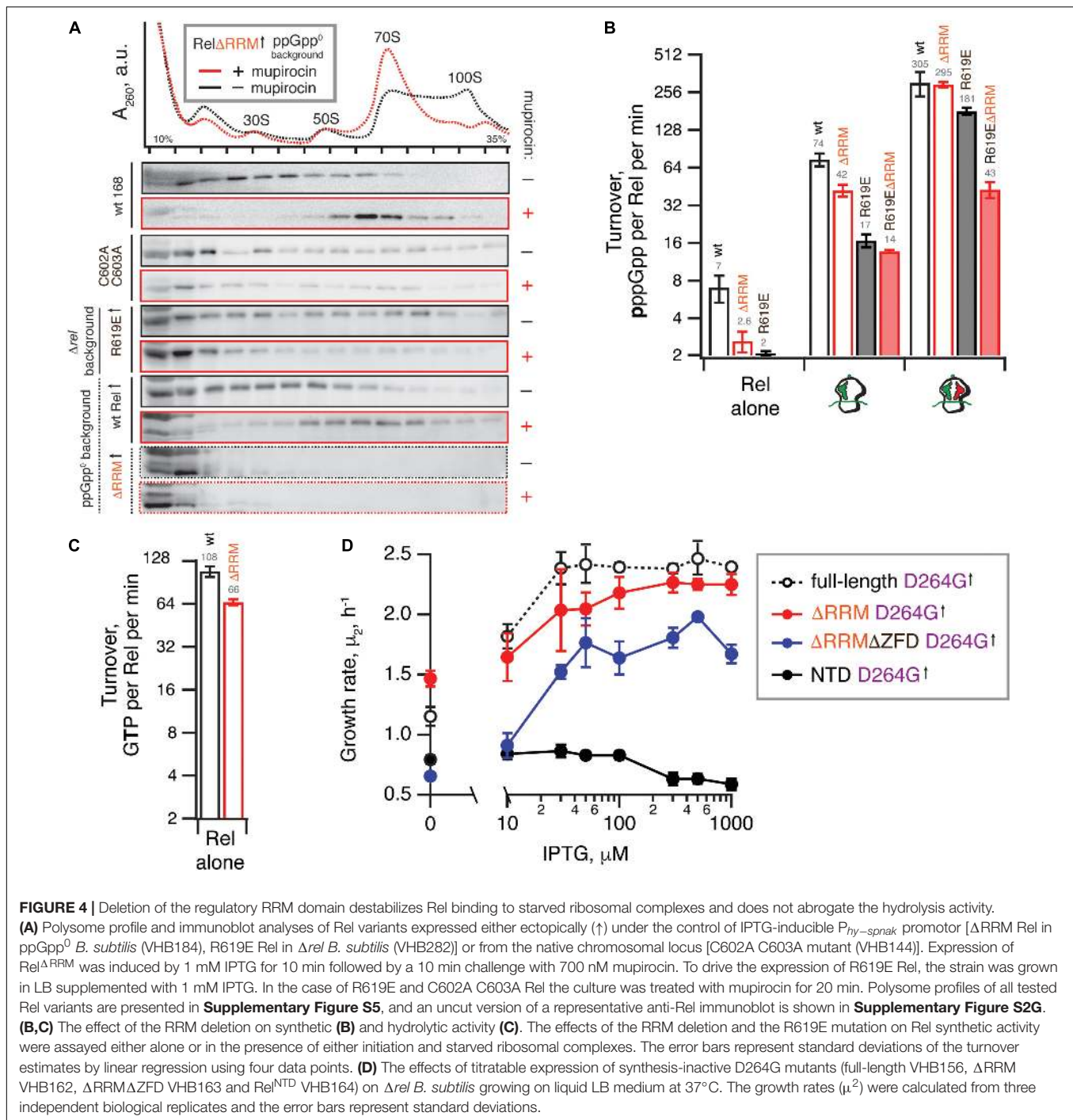
E. coli RelA activation by starved ribosomal complexes (Parker et al., 1976; Wendrich et al., 2002; Shyp et al., 2012) as well as for cellular functionality of *C. crescentus* Rel (Boutte and Crosson, 2011). The ppGpp⁰ strain expressing H420E Rel fails to grow on the minimum media, reinforcing the crucial role of that this residue, while the C602A C603A can sustain the growth, suggesting that this substitution does not completely abrogate the activity.

RRM Deletion and ZFD Mutations Destabilize *B. subtilis* Rel Binding to Starved Ribosomal Complexes

Next, we probed the ribosomal association of ΔRRM and full-length Rel expressed in the ppGpp⁰ background using a centrifugation sucrose gradient followed by Western blotting using antiserum against native, untagged *B. subtilis* Rel (**Figure 4A**). Since deacylated tRNA promotes ribosomal recruitment of *E. coli* RelA (Agirrezabala et al., 2013; Kudrin et al., 2017), we probed the association of wild type and mutant Rel variants with the ribosome both under exponential growth and upon acute isoleucine starvation induced by the isoleucyl tRNA synthetase inhibitor antibiotic mupirocin (pseudomonic acid) (Thomas et al., 2010). In good agreement with the cryo-EM structures detailing multiple contacts between the RRM and the starved complex and therefore suggesting an importance of this element in ribosomal recruitment (Arenz et al., 2016; Brown et al., 2016; Loveland et al., 2016), we do not detect a stable association of ΔRRM Rel with the ribosome upon a mupirocin challenge. This suggests that the interaction with the ribosome is significantly destabilized in Rel ^{ΔRRM} and the protein dissociates during centrifugation. It is noteworthy that, despite an unstable association of Rel ^{ΔRRM} with starved ribosomes, the expression of this protein strongly induces the accumulation of 100S ribosomal dimers, which is indicative of (p)ppGpp overproduction (Tagami et al., 2012). Note that the 100S formation is abrogated when the culture is treated with mupirocin (**Figure 4A** and **Supplementary Figure S5B**), most likely due to complete inhibition of translation by the antibiotic hindering expression of the 100S-promoting Hibernation Promoting Factor (HPF) which, in turn, is induced by accumulation of (p)ppGpp (Tagami et al., 2012).

Our microbiological experiments demonstrate that both the C602A and C603A double substitution and the R619E point substitution render Rel ^{ΔRRM} non-toxic (**Figure 3D**), which we attribute to further destabilization of Rel's interaction with starved ribosomal complexes. To directly probe the effects of these mutations, we used centrifugation experiments with full-length Rel carrying the substitutions. As expected, both the C602A C603A double mutant and R619E full-length variants are compromised in recruitment to the ribosome upon a mupirocin challenge (**Figure 4A**).

Taken together, these results demonstrate that Rel ^{ΔRRM} is significantly more toxic than the full-length protein and this toxicity is dependent on the interaction with starved ribosomes, which is, in turn, destabilized in this truncation. As a next step, we set out to test the effects of RRM deletion – either alone or in combination with mutations further compromising the

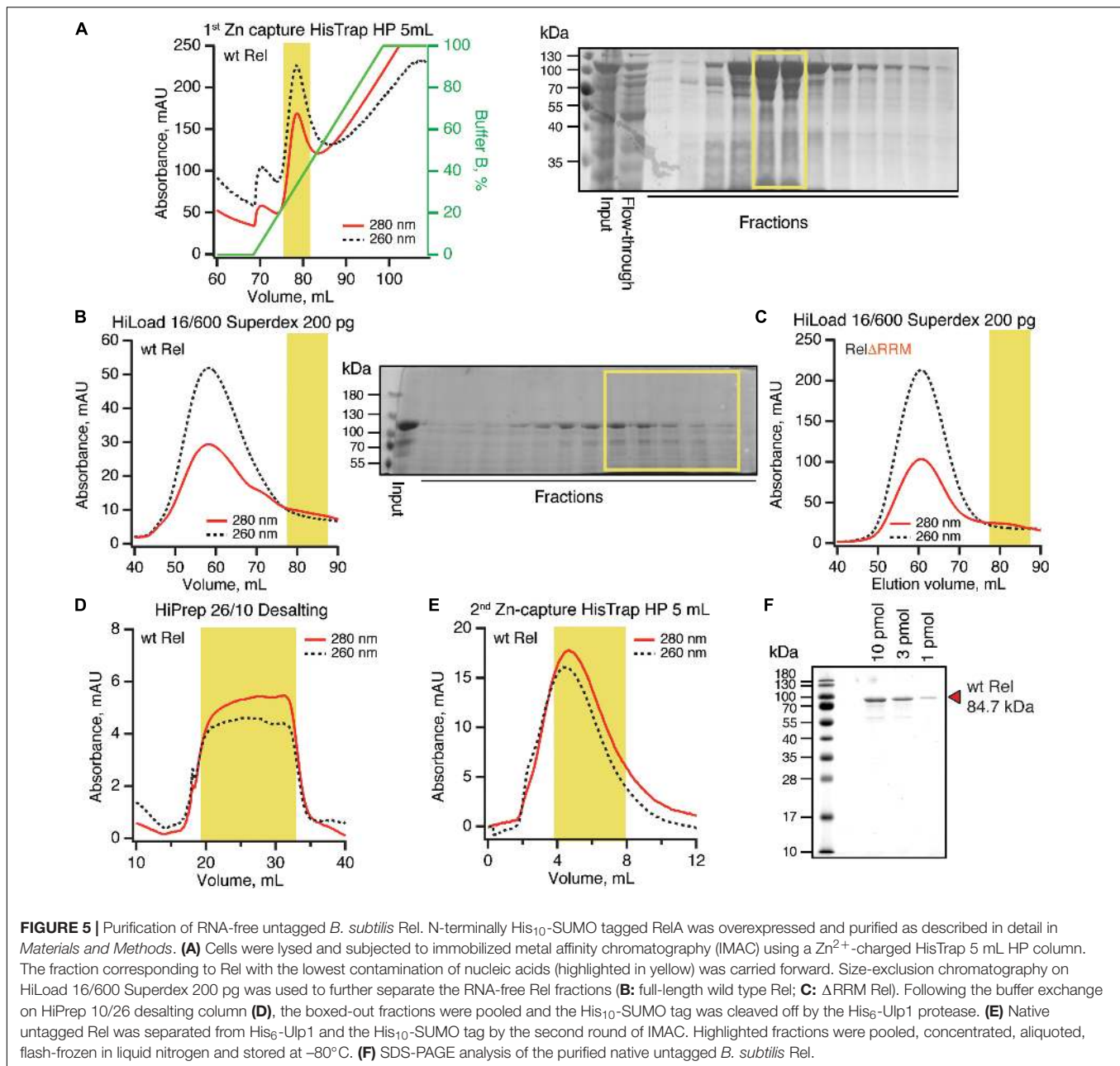


interactions with starved ribosomes – on Rel's enzymatic activity in a reconstituted *B. subtilis* biochemical system.

Purification of RNA-Free Untagged *B. subtilis* Rel Requires Size-Exclusion Chromatography

To purify untagged *B. subtilis* Rel we combined our protocols used for purification of *E. coli* RelA (Turnbull et al., 2019)

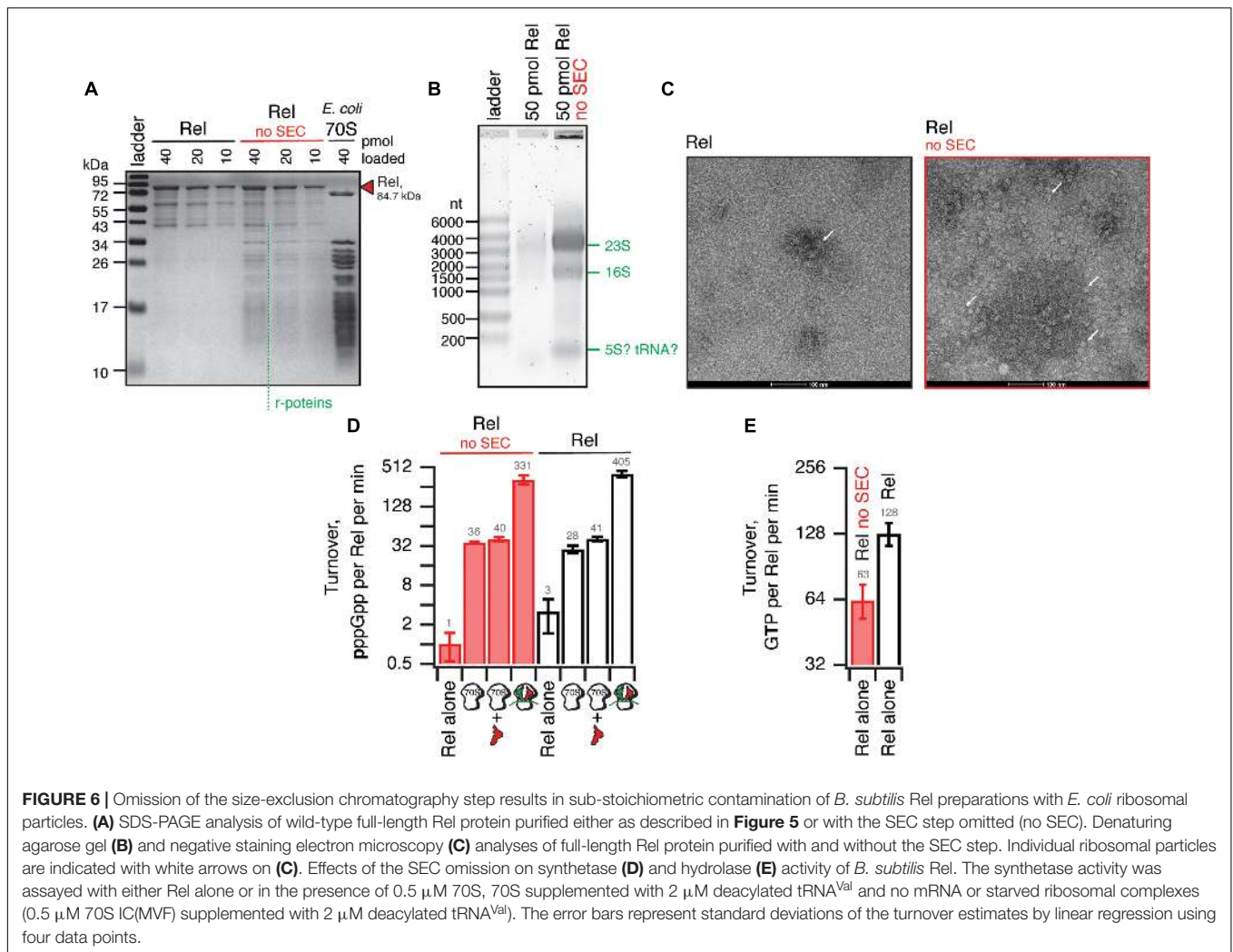
and *T. thermophilus* Rel (Van Nerom et al., 2019) (Figure 5). Importantly, during all of the chromatography steps we followed both absorbance at 260 and 280 nm complemented with SDS PAGE analysis of fractions. This is essential in order to identify and specifically pool the fractions containing Rel free from RNA contamination. After the initial capture using immobilized metal affinity chromatography (IMAC) in high ionic strength conditions (750 mM KCl) using HisTrap HP column charged with Zn $^{2+}$ in order to avoid possible replacement of the Zn $^{2+}$



in the ZFD domain by Ni²⁺ ions (Block et al., 2009), His₁₀-SUMO-Rel was applied on size-exclusion chromatography (SEC) on HiLoad 16/600 Superdex 200 pg column (Figure 5D). Both in the case of the full length (Figure 5B) and Δ RRM Rel (Figure 5C), the RNA-free fractions constitute the minority of the protein that elute considerably later than the bulk of the RNA-contaminated Rel. While the SEC step is essential for generating RNA-free Rel preparations, the majority of the protein prep is lost at this stage. After the SEC step, the buffer was exchanged to storage buffer containing arginine and glutamic acid that improve protein solubility and long-term stability (Golovanov et al., 2004) (Figure 5D), His₁₀-SUMO tag was cleaved off and removed by passing the protein via second IMAC (Figure 5E). The quality

of the final preparations was assessed by SDS-PAGE (Figure 5F and Supplementary Figure S6) as well as spectrophotometrically: OD₂₆₀/OD₂₈₀ ratio below 0.8 corresponding to less than 5% RNA contamination (Layne, 1957).

We have tested the effects of omission of the SEC step on the purification and activity of *B. subtilis* Rel preparations. Without the SEC step, the OD₂₆₀/OD₂₈₀ ratio was dramatically higher (1.9), suggesting that, counterintuitively, the ‘no SEC’ Rel preparation predominantly contains not protein but RNA. We have resolved the sample on 15% SDS-PAGE (Figure 6A) and denaturing 1.2% agarose (2% formaldehyde) (Figure 6B) gels, as well as subjected the samples to negative staining electron microscopy (Figure 6C). While the SDS-PAGE gel revealed



multiple protein bands with Mw between 40 and 10 kDa, the agarose gel revealed that the RNA contaminant is dominated by three distinct populations of approximately 3000, 1500, and 100 nucleotides in length. Large (approximately 20 nm in diameter) particles are clearly visible on the negative staining EM images. Collectively, this suggests that the RNA contamination is dominated by ribosomal particles, although it is unclear whether these are intact or partially degraded. Taking into account that 1 A_{260} corresponds to 23 pmol 70S particles, we estimate that our 'no SEC' preparations contain 45 nM 70S ribosomes per 1 μM Rel, which corresponds to sub-stoichiometric contamination of 5% of Rel being in complex, and 95% free. We next tested the effects of SEC omission on the enzymatic activity of Rel. The effects are exceedingly mild. The synthetase activity is virtually unaffected; importantly, activation by deacylated tRNA remains strictly mRNA-dependent, with tRNA^{Val} inducing the enzymatic activity of 'no SEC' Rel only in the presence of 70S initiation complexes (70S IC) but not vacant 70S ribosomes (**Figure 6D**). Importantly, since ribosomes or starved complexes are added in our synthetase assays in excess over Rel (500 nM vs. 140 nM Rel), in the final reaction mixture purified ribosomes are in

approximately 100x excess over the contaminant. Finally, the hydrolase activity of 'no SEC' Rel is approximately twofold lower (**Figure 6E**), which, however, could reflect variability in preparations.

Taken together, these results suggest that in the absence of a dedicated SEC step, Rel preparations are sub-stoichiometrically contaminated with ribosomes. While the effects of this contamination on the enzymatic activities of Rel are minor, it might interfere with other assays (see section *Discussion*).

The R619E ZFD Substitution Compromises Activation of *B. subtilis* Rel ^{Δ RRM} by Starved Ribosomal Complexes

We tested the ³H-pppGpp synthesis by full-length Rel as well as Rel ^{Δ RRM}, either alone or activated by the ribosomes or starved complexes in a reconstituted system (**Figure 4B**). When the protein is tested by itself, the Rel ^{Δ RRM} mutant is less active than the full-length, suggesting that deletion of the RRM domain does not lead to the loss of auto-inhibition. While Rel ^{Δ RRM} remains

less active than the full-length when activated by initiation complexes (about twofold), in the presence of starved ribosomal complexes the two proteins are equally active. This could be explained by tRNA stabilizing Rel on the ribosome and overriding the defect caused by the removal of the RRM domain.

The R619E mutation compromises activation of the full-length Rel by the initiation complexes (more than four-fold), and the effect is less pronounced in the presence of deacylated tRNA^{Val} (less than twofold decrease in activity). Just as in the case of the RRM deletion, a possible explanation is that the deacylated tRNA strongly stimulates the binding of Rel to the ribosome and offsets the effect of the mutation R619E. When the R619E substitution is introduced into Δ RRM Rel, the combination of the two mutations destabilizing Rel binding to the ribosome results in compromised activation both by the initiation (five-fold) and starved (seven-fold) ribosomal complex. Despite several attempts we failed to generate sufficiently pure and soluble C602A C603A Rel ^{Δ RRM}, which precluded direct biochemical characterization of this mutant.

Taken together, our biochemical results demonstrate that while RRM is important in Rel recruitment to the ribosome, this domain is not absolutely essential for the activation of its (p)ppGpp synthesis activity by starved ribosomal complexes, which is consistent with the ribosome-dependent nature of the Rel ^{Δ RRM} toxicity in live cells.

The RRM Deletion Moderately Decreases the Hydrolysis Activity of *B. subtilis* Rel

It was recently proposed that the RRM domain has a stimulatory effect on the hydrolysis activity of *C. crescentus* Rel, and the loss of this regulatory mechanism explains the toxicity of the Δ RRM mutant (Ronneau et al., 2019). This hypothesis does not explain the toxicity of the Δ RRM variant of the synthesis-only RSH RelA (Figure 2 and Turnbull et al., 2019) and our microbiological experiments showing that the synthesis-defective Δ RRM D264G variant of *B. subtilis* Rel remains active as a (p)ppGpp hydrolase (Figure 3A). Importantly, the variant characterized by Ronneau et al. (2019) (*C. crescentus* Rel ^{Δ 668–719}) does not completely lack the RRM, and it is possible that the remaining beta-strand alpha-helix turn structural element was interfering with the hydrolysis activity of the construct.

Our enzymatic assays following ³H-pppGpp degradation by full-length and Rel ^{Δ RRM} show that the latter is approximately twice less active (Figure 4C). While the defect is detectable, it is quite minor. To test if the hydrolysis defect is more pronounced in the living cell, we re-tested the hydrolysis activity of synthesis-deficient SYNTH D264G full-length Rel as well as C-terminally truncated Rel variants in the Δ rel background using the growth rate (μ_2) as a proxy (Figure 4D). We modulated the expression levels by titrating the inducer, IPTG, from 10 to 1000 μ M. In good agreement with the biochemical results demonstrating a minor defect in hydrolysis caused by deletion of the RRM domain, Δ RRM D264G Rel mutant promotes the growth of Δ rel *B. subtilis* only moderately less efficiently than the full-length D264G.

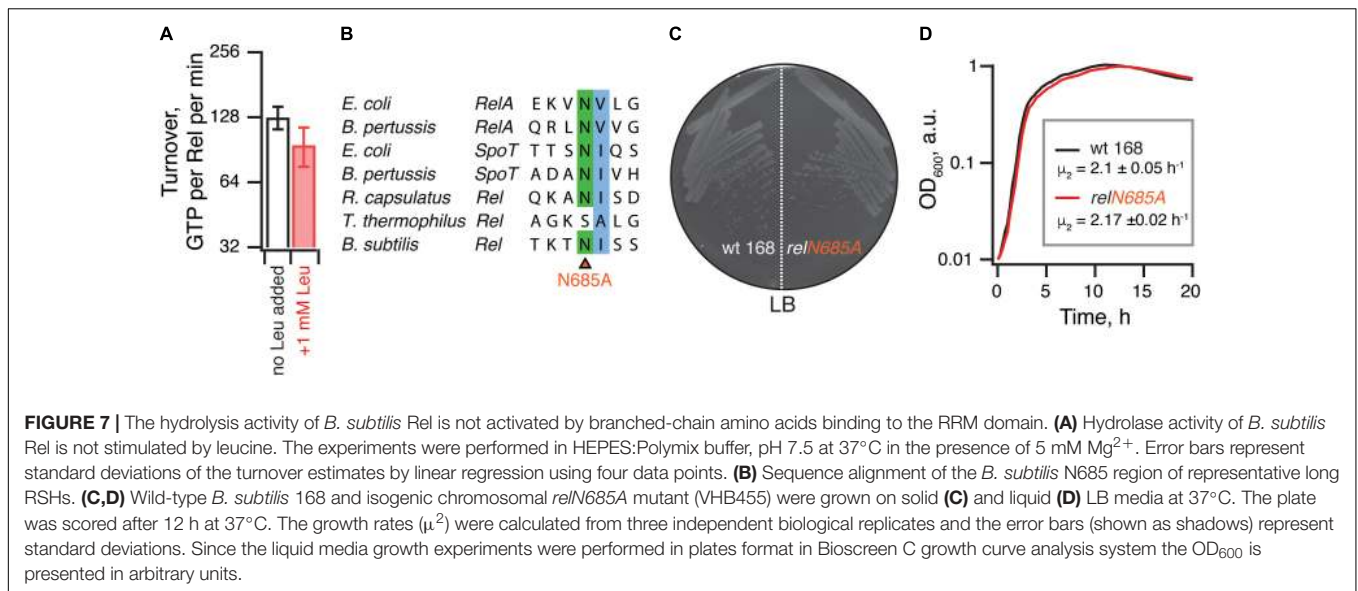
The Hydrolysis Activity of *B. subtilis* Rel Is Not Activated by Branched-Chain Amino Acids Binding to the RRM Domain

It was also recently reported that binding of branched-chain amino acids (BCAAs) to the ACT/RRM domain induces the hydrolysis activity of *Rhodobacter capsulatus* Rel (Fang and Bauer, 2018). The N651A substitution abrogates amino acid binding to *R. capsulatus* Rel^{CTD} and leads to (p)ppGpp accumulation in the cell, presumably due to lower hydrolysis activity of the mutant enzyme. It is, therefore, conceivable that *B. subtilis* Rel ^{Δ RRM} is less hydrolytically active in the cell than the full-length protein due to the loss of BCAA-mediated activation. While the *B. subtilis* Rel^{CTD} fragment was shown to preferentially bind leucine with a K_D of 225 μ M, no enzymatic assays were performed with this protein (Fang and Bauer, 2018). Notably, while the CTD region of *E. coli* RelA binds valine with high affinity (K_D of 2.85 μ M) (Fang and Bauer, 2018), this interaction could not be regulating the hydrolysis activity of this synthesis-only RSH. It is, therefore, unclear whether *B. subtilis* Rel is, indeed, regulated by branched-chain amino acids similarly to *R. capsulatus* enzyme. Therefore, we tested the effect of 1 mM leucine on ³H-pppGpp degradation by *B. subtilis* Rel. We detect no stimulatory effect (Figure 7A). Furthermore, when we introduced the N685A substitution (equivalent to N651A in *R. capsulatus*) in the chromosomal rel gene, we detected no growth defect in comparison to wild-type 168 *B. subtilis*, either on solid or liquid LB media (Figures 7B–D). Taken together, these results suggest that amino acid binding to RRM should not automatically be equated with regulation of the hydrolysis activity.

DISCUSSION

Taken together, our results demonstrate that (i) deletion of the RRM domain renders *B. subtilis* Rel and *E. coli* RelA toxic due to (p)ppGpp overproduction in a ribosome and tRNA-dependent manner, (ii) RRM deletion does not abrogate the (p)ppGpp hydrolysis activity of *B. subtilis* Rel, (iii) RRM deletion destabilizes the interaction of *B. subtilis* Rel with starved ribosomal complexes, and (iv) this destabilization renders the mutant enzyme more sensitive than the full length Rel to deactivation by additional substitutions further compromising its association with starved ribosomes. Our biochemical results do not explain why exactly Δ RRM Rel/RelA is toxic: *B. subtilis* Rel ^{Δ RRM} behaves as a weaker binder of starved ribosomal complexes (Figure 4A) and is less enzymatically active in (p)ppGpp synthesis assays (Figures 4B,C) as compared to the full-length Rel. A dedicated follow-up study is necessary to clarify this question. *E. coli* RelA ^{Δ RRM} displays a similar – although more pronounced – defect in activation by starved ribosomal complexes (Takada et al., 2020).

Our report expands the mutation toolbox for dissecting the molecular mechanisms of long RSH enzymes. We confirm that, as was shown for H432E *E. coli* RelA mutant (Winther et al., 2018), the corresponding H420E mutation in *B. subtilis* Rel is a useful tool for specifically abrogating activation of Rel by starved



ribosomal complexes. Additionally, we demonstrate the utility of two novel mutations in the ZFD domain: R619E (R629E in *E. coli* RelA) as well as a double C602A C603A substitution (C612A C613A in *E. coli* RelA). While these mutations do not completely abrogate the activation, acting in epistasis they can be employed to reveal weaker phenotypes or effects, as was shown in the current work when the mutations were combined with RRM/ACT deletion.

Finally, we would like to draw the attention of the research community working on long RSH enzymes to technical aspects of protein purification. It is common to purify Rel/RelA for biochemical experiments using a single-step purification [for example (Wood et al., 2019)]. However, both RelA (Turnbull et al., 2019) and Rel have a strong tendency for RNA contamination and multiple additional steps are necessary to remove this contaminant. Therefore, reporting the 260/280 absorbance ratio of the final preparations is essential. RNA-free protein preparations typically have a 260/280 absorbance ratio of 0.57, but this parameter can vary depending on the amino acid composition, specifically the abundance of tryptophan and phenylalanine (Layne, 1957). Without extra steps to remove RNA contamination, single-step preparations are likely to be heavily contaminated with ribosomal particles (Figure 6), which is likely to interfere with the estimation of the oligomerization state of Rel, since the RNA-bound protein elutes much earlier than the RNA-free fraction (Figures 5B,C). This contamination may explain the surprising observation that the addition of Ni-NTA purified *S. aureus* Rel inhibits the 50S assembly factor DEAD-box RNA helicase CshA (Wood et al., 2019). The unlabeled contaminating ribosomal particles could potentially be recognized by CshA, thus acting as a competitor in the helicase assay that uses a synthetic Cy3-labeled RNA duplex as a substrate. It is also plausible that formation of stable complexes of Rel with ribosomes in live *E. coli* could generate false-positive signals in bacterial two-hybrid assays, accounting for the observed protein-protein interaction between

S. aureus Rel and the ribosome assembly factors Era and CshA (Wood et al., 2019).

DATA AVAILABILITY STATEMENT

The datasets generated for this study are available on request to the corresponding author.

AUTHOR CONTRIBUTIONS

HT conceived the study. HT, MR, and VH designed the experiments. HT performed the experiments with *B. subtilis* Rel. ID and MR performed the experiments with *E. coli* RelA. VM performed the electron microscopy. RM and GA contributed tools and reagents. GCA and AG-P performed the structure and sequence analyses. HT and VH drafted and revised the manuscript with contributions from MR, AG-P, and GCA. All authors have read and approved the final version of this manuscript.

FUNDING

This work was supported by the European Regional Development Fund through the Centre of Excellence for Molecular Cell Technology (VH), the Molecular Infection Medicine Sweden (MIMS) (VH), Swedish Research Council (Grant Nos 2017-03783 to VH and 2015-04746 to GCA), Ragnar Söderberg Foundation (VH), Umeå Centre for Microbial Research (UCMR) (postdoctoral grant 2017 to HT), MIMS Excellence by Choice Postdoctoral Fellowship Programme (MR), the Fonds National de la Recherche Scientifique (Grant Nos FRFS-WELBIO CR-2017S-03, FNRS CDR J.0068.19, and FNRS-PDR T.0066.18 to AG-P) and the Fonds Jean Brachet and the Fondation Van Buuren (AG-P).

ACKNOWLEDGMENTS

We would like to thank the Protein Expertise Platform (PEP) at Umeå University and Mikael Lindberg for constructing pET24d:*His*₁₀-*SUMO*-based expression constructs and purifying His₆-Ulp1, we would also like to thank Tetiana Brodiazhenko for construction of the pMG25-based RelA and SpoT plasmids, and Julien Caballero-Montes for comments on the manuscript. The manuscript was deposited as a preprint to bioRxiv (Takada et al., 2019). The electron microscopy data was collected at the Umeå Core Facility for Electron Microscopy,

a node of the Cryo-EM Swedish National Facility, funded by the Knut and Alice Wallenberg, Family Erling Persson and Kempe Foundations, SciLifeLab, Stockholm University, and Umeå University.

SUPPLEMENTARY MATERIAL

The Supplementary Material for this article can be found online at: <https://www.frontiersin.org/articles/10.3389/fmicb.2020.00277/full#supplementary-material>

REFERENCES

- Agirrezabala, X., Fernandez, I. S., Kelley, A. C., Carton, D. G., Ramakrishnan, V., and Valle, M. (2013). The ribosome triggers the stringent response by RelA via a highly distorted tRNA. *EMBO Rep.* 14, 811–816. doi: 10.1038/embor.2013.106
- Akanuma, G., Kazo, Y., Tagami, K., Hiraoka, H., Yano, K., Suzuki, S., et al. (2016). Ribosome dimerization is essential for the efficient regrowth of *Bacillus subtilis*. *Microbiology* 162, 448–458. doi: 10.1099/mic.0.000234
- Antoun, A., Pavlov, M. Y., Tenson, T., and Ehrenberg, M. M. (2004). Ribosome formation from subunits studied by stopped-flow and Rayleigh light scattering. *Biol. Proced. Online* 6, 35–54. doi: 10.1251/bpo71
- Arenz, S., Abdelshahid, M., Sohmen, D., Payoe, R., Starosta, A. L., Berninghausen, O., et al. (2016). The stringent factor RelA adopts an open conformation on the ribosome to stimulate ppGpp synthesis. *Nucleic Acids Res.* 44, 6471–6481. doi: 10.1093/nar/gkw470
- Atkinson, G. C., Tenson, T., and Haurlyliuk, V. (2011). The RelA/SpoT homolog (RSH) superfamily: distribution and functional evolution of ppGpp synthetases and hydrolases across the tree of life. *PLoS One* 6:e23479. doi: 10.1371/journal.pone.0023479
- Avarbock, A., Avarbock, D., Teh, J. S., Buckstein, M., Wang, Z. M., and Rubin, H. (2005). Functional regulation of the opposing (p)ppGpp synthetase/hydrolase activities of RelMtb from *Mycobacterium tuberculosis*. *Biochemistry* 44, 9913–9923. doi: 10.1021/bi0505316
- Avarbock, D., Avarbock, A., and Rubin, H. (2000). Differential regulation of opposing RelMtb activities by the aminoacylation state of a tRNA. ribosome. mRNA. RelMtb complex. *Biochemistry* 39, 11640–11648. doi: 10.1021/bi001256k
- Beljantseva, J., Kudrin, P., Andresen, L., Shingler, V., Atkinson, G. C., Tenson, T., et al. (2017). Negative allosteric regulation of *Enterococcus faecalis* small alarmone synthetase RelQ by single-stranded RNA. *Proc. Natl. Acad. Sci. U.S.A.* 114, 3726–3731. doi: 10.1073/pnas.1617868114
- Block, H., Maertens, B., Spriestersbach, A., Brinker, N., Kubicek, J., Fabis, R., et al. (2009). Immobilized-metal affinity chromatography (IMAC): a review. *Methods Enzymol.* 463, 439–473. doi: 10.1016/S0076-6879(09)63027-5
- Boutte, C. C., and Crosson, S. (2011). The complex logic of stringent response regulation in *Caulobacter crescentus*: starvation signalling in an oligotrophic environment. *Mol. Microbiol.* 80, 695–714. doi: 10.1111/j.1365-2958.2011.07602.x
- Britton, R. A., Eichenberger, P., Gonzalez-Pastor, J. E., Fawcett, P., Monson, R., Losick, R., et al. (2002). Genome-wide analysis of the stationary-phase sigma factor (sigma-H) regulon of *Bacillus subtilis*. *J. Bacteriol.* 184, 4881–4890. doi: 10.1128/jb.184.17.4881-4890.2002
- Brodiazhenko, T., Johansson, M. J. O., Takada, H., Nissan, T., Haurlyliuk, V., and Murina, V. (2018). Elimination of ribosome inactivating factors improves the efficiency of *Bacillus subtilis* and *Saccharomyces cerevisiae* cell-free translation systems. *Front. Microbiol.* 9:3041. doi: 10.3389/fmicb.2018.03041
- Brown, A., Fernandez, I. S., Gordiyenko, Y., and Ramakrishnan, V. (2016). Ribosome-dependent activation of stringent control. *Nature* 534, 277–280. doi: 10.1038/nature17675
- Dalebroux, Z. D., Svensson, S. L., Gaynor, E. C., and Swanson, M. S. (2010). ppGpp conjures bacterial virulence. *Microbiol. Mol. Biol. Rev.* 74, 171–199. doi: 10.1128/MMBR.00046-09
- Dalebroux, Z. D., and Swanson, M. S. (2012). ppGpp: magic beyond RNA polymerase. *Nat. Rev. Microbiol.* 10, 203–212. doi: 10.1038/nrmicro2720
- Fang, M., and Bauer, C. E. (2018). Regulation of stringent factor by branched-chain amino acids. *Proc. Natl. Acad. Sci. U.S.A.* 115, 6446–6451. doi: 10.1073/pnas.1803220115
- Geiger, T., Kastle, B., Gratani, F. L., Goerke, C., and Wolz, C. (2014). Two small (p)ppGpp synthetases in *Staphylococcus aureus* mediate tolerance against cell envelope stress conditions. *J. Bacteriol.* 196, 894–902. doi: 10.1128/JB.01201-13
- Golovanov, A. P., Hautbergue, G. M., Wilson, S. A., and Lian, L. Y. (2004). A simple method for improving protein solubility and long-term stability. *J. Am. Chem. Soc.* 126, 8933–8939. doi: 10.1021/ja049297h
- Gratani, F. L., Horvatek, P., Geiger, T., Borisova, M., Mayer, C., Grin, I., et al. (2018). Regulation of the opposing (p)ppGpp synthetase and hydrolase activities in a bifunctional RelA/SpoT homologue from *Staphylococcus aureus*. *PLoS Genet.* 14:e1007514. doi: 10.1371/journal.pgen.1007514
- Gropp, M., Strausz, Y., Gross, M., and Glaser, G. (2001). Regulation of *Escherichia coli* RelA requires oligomerization of the C-terminal domain. *J. Bacteriol.* 183, 570–579. doi: 10.1128/jb.183.2.570-579.2001
- Haseltine, W. A., and Block, R. (1973). Synthesis of guanosine tetra- and pentaphosphate requires the presence of a codon-specific, uncharged transfer ribonucleic acid in the acceptor site of ribosomes. *Proc. Natl. Acad. Sci. U.S.A.* 70, 1564–1568. doi: 10.1073/pnas.70.5.1564
- Haurlyliuk, V., Atkinson, G. C., Murakami, K. S., Tenson, T., and Gerdes, K. (2015). Recent functional insights into the role of (p)ppGpp in bacterial physiology. *Nat. Rev. Microbiol.* 13, 298–309. doi: 10.1038/nrmicro3448
- Inabe, T. (2005). Mellite anions: unique anionic component with supramolecular self-organizing properties. *J. Mater. Chem.* 15, 1317–1328.
- Jiang, M., Sullivan, S. M., Wout, P. K., and Maddock, J. R. (2007). G-protein control of the ribosome-associated stress response protein SpoT. *J. Bacteriol.* 189, 6140–6147. doi: 10.1128/jb.00315-07
- Jimmy, S., Saha, C. K., Stavropoulos, C., Garcia-Pino, A., Haurlyliuk, V., and Atkinson, G. C. (2019). Discovery of small alarmone synthetases and their inhibitors as toxin-antitoxin loci. *bioRxiv* [Preprint]. doi: 10.1101/575399
- Katoh, K., and Standley, D. M. (2013). MAFFT multiple sequence alignment software version 7: improvements in performance and usability. *Mol. Biol. Evol.* 30, 772–780. doi: 10.1093/molbev/mst010
- Kudrin, P., Dzhygyr, I., Ishiguro, K., Beljantseva, J., Maksimova, E., Oliveira, S. R. A., et al. (2018). The ribosomal A-site finger is crucial for binding and activation of the stringent factor RelA. *Nucleic Acids Res.* 46, 1973–1983. doi: 10.1093/nar/gky023
- Kudrin, P., Varik, V., Oliveira, S. R., Beljantseva, J., Del Peso Santos, T., Dzhygyr, I., et al. (2017). Subinhibitory concentrations of bacteriostatic antibiotics induce *relA*-dependent and *relA*-independent tolerance to beta-Lactams. *Antimicrob. Agents Chemother.* 61:e02173-16. doi: 10.1128/AAC.02173-16
- Kushwaha, G. S., Oyeyemi, B. F., and Bhavesh, N. S. (2019). Stringent response protein as a potential target to intervene persistent bacterial infection. *Biochimie* 165, 67–75. doi: 10.1016/j.biochi.2019.07.006
- Layne, E. (1957). Spectrophotometric and turbidimetric methods for measuring proteins. *Methods Enzymol.* 3, 447–454. doi: 10.1016/S0076-6879(57)03413-8
- Liu, K., Bittner, A. N., and Wang, J. D. (2015). Diversity in (p)ppGpp metabolism and effectors. *Curr. Opin. Microbiol.* 24, 72–79. doi: 10.1016/j.mib.2015.01.012

- Loveland, A. B., Bah, E., Madireddy, R., Zhang, Y., Brilot, A. F., Grigorieff, N., et al. (2016). Ribosome*RelA structures reveal the mechanism of stringent response activation. *eLife* 5:e17029. doi: 10.7554/eLife.17029
- Mechold, U., Murphy, H., Brown, L., and Cashel, M. (2002). Intramolecular regulation of the opposing (p)ppGpp catalytic activities of Rel(Seq), the Rel/Spo enzyme from *Streptococcus equisimilis*. *J. Bacteriol.* 184, 2878–2888. doi: 10.1128/jb.184.11.2878-2888.2002
- Mittenhuber, G. (2001). Comparative genomics and evolution of genes encoding bacterial (p)ppGpp synthetases/hydrolases (the Rel, RelA and SpoT proteins). *J. Mol. Microbiol. Biotechnol.* 3, 585–600.
- Molin, S., Stougaard, P., Uhlin, B. E., Gustafsson, P., and Nordstrom, K. (1979). Clustering of genes involved in replication, copy number control, incompatibility, and stable maintenance of the resistance plasmid R1drd-19. *J. Bacteriol.* 138, 70–79. doi: 10.1128/jb.138.1.70-79.1979
- Murina, V., Kasari, M., Haurlyliuk, V., and Atkinson, G. C. (2018a). Antibiotic resistance ABCF proteins reset the peptidyl transferase centre of the ribosome to counter translational arrest. *Nucleic Acids Res.* 46, 3753–3763. doi: 10.1093/nar/gky050
- Murina, V., Kasari, M., Takada, H., Hinno, M., Saha, C. K., Grimshaw, J. W., et al. (2018b). ABCF ATPases involved in protein synthesis, ribosome assembly and antibiotic resistance: structural and functional diversification across the tree of life. *J. Mol. Biol.* 431, 3568–3590. doi: 10.1016/j.jmb.2018.12.013
- Nanamiya, H., Kasai, K., Nozawa, A., Yun, C. S., Narisawa, T., Murakami, K., et al. (2008). Identification and functional analysis of novel (p)ppGpp synthetase genes in *Bacillus subtilis*. *Mol. Microbiol.* 67, 291–304. doi: 10.1111/j.1365-2958.2007.06018.x
- Parker, J., Watson, R. J., and Friesen, J. D. (1976). A relaxed mutant with an altered ribosomal protein L11. *Mol. Gen. Genet.* 144, 111–114. doi: 10.1007/bf00277313
- Ronneau, S., Caballero-Montes, J., Coppine, J., Mayard, A., Garcia-Pino, A., and Hallez, R. (2019). Regulation of (p)ppGpp hydrolysis by a conserved archetypal regulatory domain. *Nucleic Acids Res.* 47, 843–854. doi: 10.1093/nar/gky1201
- Schreiber, G., Metzger, S., Aizenman, E., Roza, S., Cashel, M., and Glaser, G. (1991). Overexpression of the relA gene in *Escherichia coli*. *J. Biol. Chem.* 266, 3760–3767.
- Shyp, V., Tankov, S., Ermakov, A., Kudrin, P., English, B. P., Ehrenberg, M., et al. (2012). Positive allosteric feedback regulation of the stringent response enzyme RelA by its product. *EMBO Rep.* 13, 835–839. doi: 10.1038/embor.2012.106
- Spizizen, J. (1958). Transformation of biochemically deficient strains of *Bacillus subtilis* by deoxyribonucleate. *Proc. Natl. Acad. Sci. U.S.A.* 44, 1072–1078. doi: 10.1073/pnas.44.10.1072
- Steinchen, W., and Bange, G. (2016). The magic dance of the alarmones (p)ppGpp. *Mol. Microbiol.* 101, 531–544. doi: 10.1111/mmi.13412
- Tagami, K., Nanamiya, H., Kazo, Y., Maehashi, M., Suzuki, S., Namba, E., et al. (2012). Expression of a small (p)ppGpp synthetase, YwaC, in the (p)ppGpp(0) mutant of *Bacillus subtilis* triggers YvyD-dependent dimerization of ribosome. *Microbiologyopen* 1, 115–134. doi: 10.1002/mbo3.16
- Takada, H., Roghanian, M., Caballero-Montes, J., Van Nerom, K., Jimmy, S., Kudrin, P., et al. (2020). Ribosome association primes the stringent factor Rel for recruitment of deacylated tRNA to ribosomal A-site. *bioRxiv* [Preprint]. doi: 10.1101/2020.01.17.910273
- Takada, H., Roghanian, M., Murina, V., Dzhygyr, I., Murayama, R., Akanuma, G., et al. (2019). The C-terminal RRM/ACT domain is crucial for fine-tuning the activation of 'long' RelA-SpoT Homolog enzymes by ribosomal complexes. *bioRxiv* [Preprint]. doi: 10.1101/849810
- Tamman, H., Van Nerom, K., Takada, H., Vandenberg, S., Polikanov, Y., Hofkens, J., et al. (2019). Nucleotide-mediated allosteric regulation of bifunctional Rel enzymes. *bioRxiv* [Preprint]. doi: 10.1101/670703
- Thomas, C. M., Hothersall, J., Willis, C. L., and Simpson, T. J. (2010). Resistance to and synthesis of the antibiotic mupirocin. *Nat. Rev. Microbiol.* 8, 281–289. doi: 10.1038/nrmicro2278
- Turnbull, K. J., Dzhygyr, I., Lindemose, S., Haurlyliuk, V., and Roghanian, M. (2019). Intramolecular interactions dominate the autoregulation of *Escherichia coli* stringent factor RelA. *Front. Microbiol.* 10:1966. doi: 10.3389/fmicb.2019.01966
- Van Nerom, K., Tamman, H., Takada, H., Haurlyliuk, V., and Garcia-Pino, A. (2019). The Rel stringent factor from *Thermus thermophilus*: crystallization and X-ray analysis. *Acta Crystallogr. F Struct. Biol. Commun.* 75, 561–569. doi: 10.1107/S2053230X19010628
- Waterhouse, A. M., Procter, J. B., Martin, D. M., Clamp, M., and Barton, G. J. (2009). Jalview Version 2—a multiple sequence alignment editor and analysis workbench. *Bioinformatics* 25, 1189–1191. doi: 10.1093/bioinformatics/btp033
- Wendrich, T. M., Blaha, G., Wilson, D. N., Marahiel, M. A., and Nierhaus, K. H. (2002). Dissection of the mechanism for the stringent factor RelA. *Mol. Cell* 10, 779–788. doi: 10.1016/s1097-2765(02)00656-1
- Wilkinson, R. C., Batten, L. E., Wells, N. J., Oyston, P. C., and Roach, P. L. (2015). Biochemical studies on *Francisella tularensis* RelA in (p)ppGpp biosynthesis. *Biosci. Rep.* 35:e00268. doi: 10.1042/BSR20150229
- Winther, K. S., Roghanian, M., and Gerdes, K. (2018). Activation of the stringent response by loading of RelA-tRNA complexes at the ribosomal A-site. *Mol. Cell* 70, 95–105.e4. doi: 10.1016/j.molcel.2018.02.033
- Wood, A., Irving, S. E., Bennison, D. J., and Corrigan, R. M. (2019). The (p)ppGpp-binding GTPase Era promotes rRNA processing and cold adaptation in *Staphylococcus aureus*. *PLoS Genet.* 15:e1008346. doi: 10.1371/journal.pgen.1008346
- Xiao, H., Kalman, M., Ikehara, K., Zemel, S., Glaser, G., and Cashel, M. (1991). Residual guanosine 3',5'-bispyrophosphate synthetic activity of relA null mutants can be eliminated by spoT null mutations. *J. Biol. Chem.* 266, 5980–5990.
- Yang, N., Xie, S., Tang, N. Y., Choi, M. Y., Wang, Y., and Watt, R. M. (2019). The Ps and Qs of alarmone synthesis in *Staphylococcus aureus*. *PLoS One* 14:e0213630. doi: 10.1371/journal.pone.0213630

Conflict of Interest: The authors declare that the research was conducted in the absence of any commercial or financial relationships that could be construed as a potential conflict of interest.

Copyright © 2020 Takada, Roghanian, Murina, Dzhygyr, Murayama, Akanuma, Atkinson, Garcia-Pino and Haurlyliuk. This is an open-access article distributed under the terms of the Creative Commons Attribution License (CC BY). The use, distribution or reproduction in other forums is permitted, provided the original author(s) and the copyright owner(s) are credited and that the original publication in this journal is cited, in accordance with accepted academic practice. No use, distribution or reproduction is permitted which does not comply with these terms.